Calcium alginate beads reinforced with synthetic oligomers, linear polyethylenimine and Cu(II): structural stability and potential applications

Dimas Ignacio Torres, María Emilia Villanueva, Juan Manuel Lázaro-Martínez, Guillermo Javier Copello & Viviana Campo Dall' Orto

Cellulose

ISSN 0969-0239
Volume 25
Number 3

Cellulose (2018) 25:1657-1672
DOI 10.1007/s10570-018-1684-8

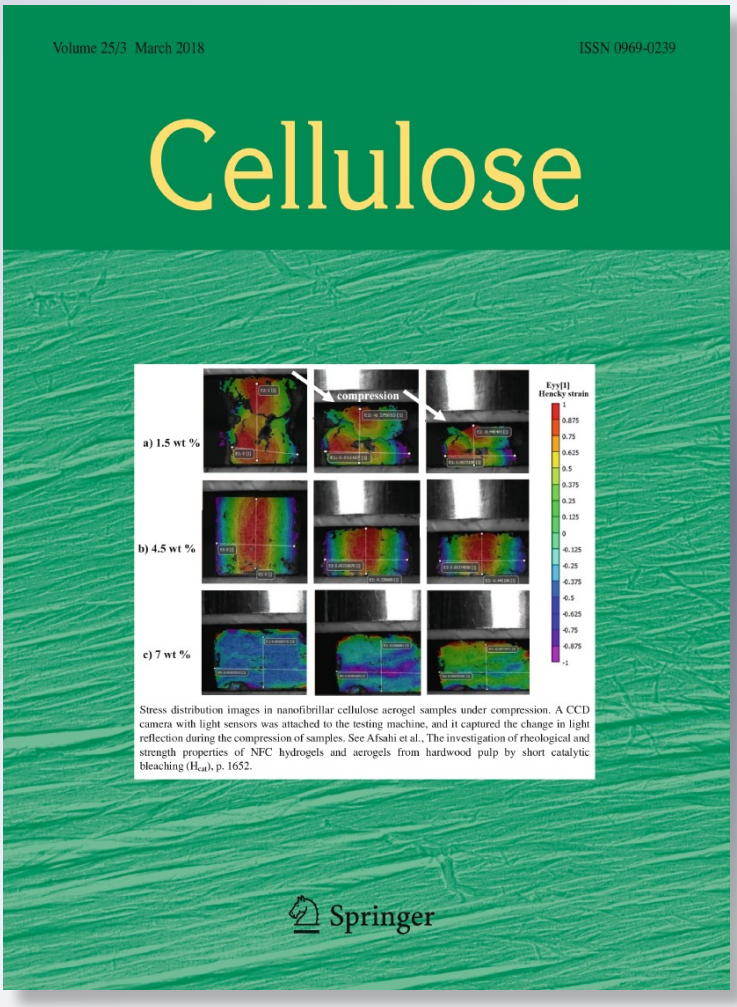

Stress distribution images in nanofibrillar cellulose aerogel samples under compression. A CCD camera with light sensors was attached to the testing machine, and it captured the change in light reflection during the compression of samples. See Afsahi et al., The investigation of rheological and strength properties of NFC hydrogels and aerogels from hardwood pulp by short catalytic bleaching (H_{cat}), p. 1652.

Springer

Cellulose (2018) 25:1657–1672
https://doi.org/10.1007/s10570-018-1684-8

ORIGINAL PAPER

Calcium alginate beads reinforced with synthetic oligomers, linear polyethylenimine and Cu(II): structural stability and potential applications

Dimas Ignacio Torres · María Emilia Villanueva · Juan Manuel Lázaro-Martínez · Guillermo Javier Copello · Viviana Campo Dall' Orto

Received: 13 October 2017 / Accepted: 29 January 2018 / Published online: 13 February 2018

Abstract Calcium alginate beads were reinforced with linear polyethylenimine (PEI), Cu(II) and synthetic oligomers derived from a diepoxide, methacrylic acid and imidazole, to increase the resistance to stirring and vibration for environmental applications. The FT-IR and Raman spectra of the beads confirmed the presence of the organic reactants and their interactions. The SEM images of the lyophilized beads with an excess of oligomers exhibited an ordered core structure surrounded by a shell. The elemental mapping by EDAX showed a homogeneous distribution of Ca(II) and Cu(II), and a density influenced by PEI. The beads more resistant to sonication were those with the highest oligomer content. The enzyme soybean peroxidase (SBP) was immobilized in the beads for an environmental application that requires a stable matrix from chemical and structural points of view. The synergistic action of the entrapped SBP and Cu(II) on H_2O_2 activation induced the removal of an azo dye from aqueous solutions. Free radicals and O_2 were released from Cu(II)-sites in the presence of the peroxide. The content of the oligomers determined the efficiency of the beads on dye removal.

Keywords Alginate beads · Soybean peroxidase · Polyethylenimine · Oligomers · Raman spectroscopy · Dye decolorization

Abbreviations

DMPO	5,5-Dimethyl-1-pyrroline-N oxide (spin trap)
EDAX	Energy dispersive X-ray analysis
EGDE	Ethyleneglycol diglycidyl ether
ESR	Electronic spin resonance
FT-IR	Fourier transform infra-red spectroscopy
IM	Imidazole
MAA	Methacrylic acid
MO	Methyl orange

Electronic supplementary material The online version of this article (https://doi.org/10.1007/s10570-018-1684-8) contains supplementary material, which is available to authorized users.

D. I. Torres · M. E. Villanueva · G. J. Copello · V. Campo Dall' Orto
Departamento de Química Analítica y Fisicoquímica, Facultad de Farmacia y Bioquímica, Universidad de Buenos Aires, Buenos Aires, Argentina

D. I. Torres · M. E. Villanueva · J. M. Lázaro-Martínez · G. J. Copello (✉) · V. Campo Dall' Orto (✉)
Instituto de Química y Metabolismo del Fármaco (IQUIMEFA), CONICET-Universidad de Buenos Aires, Buenos Aires, Argentina
e-mail: gcopello@ffyb.uba.ar

V. Campo Dall' Orto
e-mail: vcdall@ffyb.uba.ar

J. M. Lázaro-Martínez
Departamento de Química Orgánica, Facultad de Farmacia y Bioquímica, Universidad de Buenos Aires, Buenos Aires, Argentina

PEI.HCl	22-kDa linear polyethylenimine hydrochloride
SBP	Soybean peroxidase
SEM	Scanning electron microscopy

Introduction

The immobilization of enzymes, microorganisms, and plant and animal cells is carried out to protect them from environmental stresses, such as acid/alkaline conditions, chemical incompatibility, wet/dry cycles, and temperature changes in bioreactor systems for catalytic processes (Kurillova et al. 2000; Kawaguti et al. 2006; Cheng et al. 2011; Xue et al. 2013). Natural polysaccharides, such as alginate, low-methoxyl pectate, and chitosan, are usually selected to build gel beads by ionotropic gelation with Ca^{2+} for the immobilization of enzymes and cells due to their innocuousness and biocompatibility (Kurillova et al. 2000; Kawaguti et al. 2006). Alginate has been thoroughly studied with this aim in spite of the poor mechanical properties of the resulting gel matrixes. Another main drawback is their instability in the presence of phosphates, citrate, tartrate and certain cations, such as Mg^{2+} or K^{+}, requiring stabilization and hardening when used continuously in complex media of catalytic processes (Kurillova et al. 2000; Kawaguti et al. 2006; Cheng et al. 2011; Xue et al. 2013).

Typically, Ca(II)-alginate beads are hollow spheres with multilayer polymeric shells that modulate the mechanical stability and the adequate permeability of solutes (Cui et al. 2014). To overcome the limitations, a variety of polymers or functionalized macromolecules were added into the bead architecture, such as polyethylenimine hydrochloride (PEI.HCl) (Nussinovitch 2010). Alternative strategies have consisted of treating the preformed Ca(II)-alginate beads with the cross-linking polyethylenimine (PEI) followed by glutaraldehyde (GA) (Kurillova et al. 2000; Kawaguti et al. 2006; Cheng et al. 2011; Xue et al. 2013).

In this context, enzyme immobilization on a suitable and insoluble support leads to the stabilization of the protein for controlled release or for heterogeneous catalysis in bioreactors, both attractive at an industrial scale (Nisha et al. 2012). The preservation of catalytic activity on thermally treated Ca(II)-alginate gels could be improved by the presence β-cyclodextrin, pectin, arabic and guar gums and/or trehalose (Santagapita et al. 2011; Traffano-Schiffo et al. 2017). The enzyme diffusion from Ca(II)-alginate gel beads through high pores could be prevented by adding gelatin (Mogharabi et al. 2012) or by glutaraldehyde fixation (Paul et al. 2014), sometimes preceded by protein aggregation (Xu and Yang 2013). With a different approach, a PEI coating was used to minimize the leakage of encapsulated aminoacylase. The SEM images of PEI-coated spheres revealed surfaces with cross-linking networks, a physical barrier presumably formed by ionic interactions of alginate groups with those of protonated PEI ($PEIH^{+}$) (Lee et al. 1993).

Although GA is one of the most studied cross-linkers, its use has received several objections due to its cytotoxicity (Reddy et al. 2015). With the aim of replacing GA, fully synthetic polymeric compounds were used in the assembly of structurally stable hydrogel microbeads and capsules (Nussinovitch 2010). Some chains are functionalized with end groups that tolerate mild, but efficient, chemical cross-linking. Poly(methylmethacrylate), polyurethane, polythiourea, poly[(ethylene oxide)-*co*-glycidol], epoxy resins and urea–formaldehyde are some examples of polymeric compounds involved in micro- and nanocapsule assemblies (Nussinovitch 2010).

Copper alginate has rarely been used as an entrapment matrix because many enzymes are inactivated by these cations. However, copper is essential for the activity of other enzymes, such as laccase (Homaei et al. 2013; Teerapatsakul et al. 2008; Le et al. 2016), tyrosinase (Ates et al. 2007) or polyphenol oxidase (Kocaturk and Yagar 2010), and can contribute to the long-term practical use of these biomolecules in the beads.

There are reports of the soybean peroxidase (SBP) enzyme extracted from the raw seed hulls and entrapped within hybrid (silica sol–gel/alginate) particles for the removal of phenols in wastewater (Trivedi et al. 2006). This enzyme was active even in the presence of Cu(II) in the entrapment matrix (Anu et al. 2016). In fact, peroxidase activity in copper-exposed culture medium and in control culture showed no significant difference (Anu et al. 2016).

With the aim of keeping the advantages of PEI and overcoming GA disadvantages, we present the study of the use of ampholytic oligomers as GA

replacement. Sodium alginate, Ca(II), PEI.HCl and Cu(II) were properly combined to impart structural and chemical stability to the beads by making use of the high cationic binding capacity of the oligomers. The compounds obtained from ethylene glycol diglycidyl ether (EGDE), imidazole (IM) and methacrylic acid (MAA), were synthesized according to a variation of a former method for ampholytes (Lombardo Lupano et al. 2016). They can interact with alginate and the cations by means of –OH and ionized functional groups, retaining the cations and preserving the bead structure and cationic functionality (Lombardo Lupano et al. 2016). Cytotoxicity assays were performed to study the safety of these novel oligomers.

The enzyme SBP was immobilized inside these gel beads for a potential environmental application that requires a stable matrix from chemical and structural points of view. The use of alternative additives to reinforce the matrix for SBP entrapment has not so far been explored. The performance of these Ca(II)/Cu(II)-alginate beads containing SBP, synthetic PEI and oligomers, was studied on an azo dye decolorization using H_2O_2 as oxidant. The cation release activity was studied with Cu(II)-hardened beads by antimicrobial activity assay.

Experimental

Chemicals and reagents

Imidazole (IM; 99 wt%), methacrylic acid (MAA; 99 wt%), ethylene glycol diglycidyl ether (EGDE; 50 wt% in ethylene glycol dimethylether), and 5,5-dimethyl-1-pyrroline *N*-oxide (DMPO) were purchased from Sigma–Aldrich. Linear polyethylenimine hydrochloride (PEI.HCl) of 22 kDa was synthesized according with previous reports (Lázaro-Martínez et al. 2015). The other reagents were analytical grade.

Sodium alginate salt was food grade, from PlusQuímica (Buenos Aires, Argentina), purity: 99.7 wt% on dry base; size mesh: 80; viscosity (1 w/v %): 632 mPa, G (glucuronic acid) wt%: 47, M/G ratio: 1.13, and Mw: 317 ± 2 kDa (polydispersity: 5.5); pH: 6.96. Loss on drying at 105° C for 4 h: 13.4 wt%, insoluble matter in water: 0.25 wt%, and ash: 25 wt%.

The Mw of sodium alginate food grade was determined by size exclusion chromatography, using a Ultrahydrogel linear column (Waters), a mobile phase containing 0.10 M $(NH_4)_2HPO_4$ and 0.30 M NaCl, and a differential refractive detector. Polyethyleneglycol (PEG) samples were used as Mw standards.

Synthesis of water-soluble EGDE-IM-MAA oligomers

This synthetic strategy is an adaptation of a former procedure described for the synthesis of ampholytes (Lombardo Lupano et al. 2016). The reaction proceeded without stirring, except when the reagents were added and needed to be mixed. In a first step, an aliquot of 6.0 g (88 mmol) of IM was dissolved in 24 mL of acetonitrile in a round-bottom flask. Then, 12 mL of EGDE (108 mmol oxirane oxygen) were added to the mixture, the end of the neck was covered with a piece of aluminum foil and it was thermostatted at 60° C for 24 h. It must be pointed out that the mixture was not deoxygenated. In a second step, 6.0 mL of MAA (71 mmol) were poured into the mixture and the reaction continued for a further 24 h at 60° C. Then, the acetonitrile was evaporated at reduced pressure, and the product was mixed with a minimum volume of distilled water to obtain solutions of 300 mg mL^{-1}, determined by weighing after lyophilization.

Cytotoxicity assays

The safety of these oligomers was tested following standard procedures with mammalian cells. The mammalian continuous cell line was derived from the kidney of an African green monkey, and Vero cells were purchased from ATCC (ATCC No: CCL-81). Cells were cultured in Dulbecco's modified Eagle's medium (Life Technologies, Carlsbad, CA, USA) supplemented with 10% fetal bovine serum (Life Technologies) and maintained at 37 °C in a humidified atmosphere of 5% CO_2.

For cytotoxicity assays, cells were seeded in 96-well plates (2.0×10^4 cells/well), grown overnight and treated with the oligomer solution at different concentrations (1.5–100 μM, or 600 μg L^{-1} to 40 mg L^{-1}). The cytotoxic activity was determined after 24 h using the 3-(4,5-dimethylthiazol-2-yl)-5-(3-carboxymethoxyphenyl)-2-(4-sulfophenyl)-2H-tetrazolium/phenazine methosulfate assay (Promega,

Madison, WI, USA). The absorbance at λ: 495 nm was determined using a FlexStation 3 (Molecular Devices, Sunnyvale, CA, USA).

Bead production

The procedure can be divided in steps:

a. Internal solution preparation: a 100-mg aliquot of sodium alginate was mixed with 10 mL of distilled water under stirring until a highly viscous solution was formed. Then, a certain volume (50, 100 or 200 μL) of EGDE-IM-MAA oligomer solution was added. At this step, the alginate solution becomes more fluid. Another 100-mg aliquot of sodium alginate was added to the previous mixture, again forming a viscous solution which was sonicated in order to eliminate air bubbles. An alternative solution without oligomers was prepared for control experiments: in this case, the sodium alginate was mixed with water and dissolved by stirring overnight.
b. Bead assembly: a 1-cm^3 syringe with a needle was used to dispense the internal solution. On the other hand, the external solution was prepared with certain mass (100, 200 or 300 mg) of linear polyethylenimine hydrochloride (PEI.HCl; 22 kDa; 3–4 polydispersity and 23 mmol of amine groups per gram) and distilled water to complete 100 mL of solution. An aliquot of 10 mL of this external solution was transferred to a glass beaker, the tip of the needle of the syringe was placed 5 cm above the surface of the solution and 1 mL of internal solution was dropped (1 drop per second) forming 80 ± 5 beads. In order to obtain an external layer of PEI with a homogeneous thickness, the medium and the beads were stirred at 20 rpm for 5 min. The beads, translucent at the start, slowly became opaque from the surface towards the core due to the reactions involving PEI, the oligomers and alginate. The beads were named OXPY according to the mass of the oligomers (X) and PEI.HCl (Y) in the internal and external assembly solutions, respectively. In that way, we worked with the following samples: O15P20, O15P30, O30P10, O30P20, O30P30, O60P20 and O60P30. The control in the absence of oligomers was named O0PY.
c. Hardening: the beads were directly transferred with the spoon of a spatula to a solution containing 40 mg of $CaCl_2$ in 10 mL, and let equilibrate for 1 h. Then, they were directly transferred to the Cu(II)-hardening solution, made of 40 mg of copper acetate monohydrate (0.20 mmol Cu(II)) in distilled water to a final volume of 10 mL, and incubated under slow stirring for 12 h. Finally, the beads were transferred and washed 3 times with distilled water for 10 min, the superficial drops were dried with a paper tissue, and they were stored in a wet chamber at 5 °C (stable for a month).

The beads for Raman spectroscopic analysis were prepared with $CaCl_2$ or $ZnCl_2$ (equivalent to 0.20 mmol of the corresponding metal ion) instead of copper acetate monohydrate in the hardening solution.

The different contact times and amounts of reagents mentioned in each step were the lowest necessary to reach the desired properties (homogeneous thickness, resistance to convection, etc.). Higher and lower times or amounts of compounds were tested in each case, and the best conditions were chosen.

The size of the beads was obtained by taking pictures of ten samples beside a length scale and measuring the diameters, which were averaged together with the standard deviation. The number of samples from a batch was selected considering a maximal relative uncertainty of 0.10 with a confidence level of 95% for the mean diameter of the beads.

Enzyme entrapment

When necessary, the encapsulation of the seed coat SBP was made by using a 13.15-mg mL^{-1} purified SBP solution (with an activity of 1551 U mL^{-1}) (Torres et al. 2017) instead of distilled water in the internal solution of the first step of bead production.

The catalytic activity of the enzyme in the purified extract was determined by comparison with the standard purchased from Sigma: peroxidase from glycine max (soybean) P-1432, 50–150 units per mg of solid. One unit will form 1.0 mg of purpurogallin from pyrogallol in 20 s at pH 6.0 at 20°C.

The activity of SBP encapsulated in the beads was estimated by the difference between the SBP activity in the internal solution used to assemble the beads and

the activity found in the external solution where the beads were formed, which corresponded to 19 U per bead.

Scanning electron microscopy (SEM) and energy dispersive X-ray analysis (EDAX)

Samples were analyzed using a Philips 505 microscope for scanning electron microscopy (SEM), while elemental analyses were carried out by using an EDAX analyzer. Each bead was dried by lyophilization and cut into two pieces with a scalpel. Then, the samples were coated with 20 nm of gold, before taking SEM and EDAX images (25 keV) from the core and shell of each bead.

FT-IR and Raman spectroscopies

ATR-FT-IR (attenuated total reflectance-Fourier transform-Infra red) with a one-reflection diamond crystal, and FT-Raman spectra of the materials were recorded using a Nicolet iS50 Advanced Spectrometer (Thermo Scientific). ATR-FT-IR spectra were recorded with 32 scans and a resolution of 4 cm^{-1}. FT-Raman spectra were acquired with an excitation laser beam of 1064 nm, 0.5-W laser power, resolution of 4 cm^{-1}, and 50 scans. All samples were previously dried for 24 h at 60° C to avoid water-related band interference.

Assays of resistance to sonication

Ten beads of each type were immersed in 5.0 mL of distilled water in a glass flask (internal diameter: 1.5 cm), and sonicated at 50° C with a frequency of 40 kHz for 120 min. Every 10 min, the number of intact beads was registered. One-way analysis of variance was used to compare the means of the experimental results.

The number of beads (ten, in this experiment) from a batch was selected considering a maximal relative uncertainty of 0.10 with a confidence level of 95% for the means of the results. Different combinations of frequency and time were assayed, and the selected values were adequate to minimize the standard deviation on intact bead counting.

Measurement of texturometric parameters

Bead texture was analyzed in a TA.XT2i Texture Analyzer (Stable Micro Systems, UK) equipped with a load cell of 5 kg and a cylindrical metal compression plate of 25 mm diameter. The texture profile analysis (TPA) consisted of two consecutive cycles of bead compression at 0.5 mm s^{-1} to 40% of the original bead height with a 2-s gap between cycles. In each assay, one bead was compressed. Data was processed with the Texture Expert® software and the textural parameters (hardness and cohesiveness) were calculated from the TPA curve of force (N) versus time (s) with the following definitions (Bourne and Comstock 1981): hardness (N) is defined as the peak force during the first compression cycle, and cohesiveness (dimensionless) as the ratio of the areas under the second and first compression (A2/A1). The results represent the mean of at least five tests.

Measurement of free radicals by electron spin resonance (ESR)

The beads were put in contact with H_2O_2 solution for the activation of this peroxide by Cu(II). The initial H_2O_2 concentration was set close to 10 mM. Ten beads were suspended in 5.00 mL of H_2O_2 solution and the production of free radicals was followed by ESR.

Aliquots of 32 μL taken at 10 min of reaction were mixed with 16 μL of 3 M DMPO (spin trap), and the continuous wave (CW) ESR spectra of the DMPO spin adducts were recorded at 20 °C, 3 min after the end of incubation (Lázaro Martínez et al. 2008), in an X-band ESR Spectrometer Bruker EMX Plus (Bruker Biospin, Germany).

The spectrometer settings were: center field: 3515 G, sweep width: 100 G, microwave power: 10 mW, microwave frequency: 9.85 GHz, conversion time: 2.56 ms, time constant: 2.56 ms, modulation frequency: 50 kHz, modulation amplitude: 0.11 G, gain: 2.00×10^4, and resolution: 1024 points. All spectra were the accumulation of 20 scans. For fitting and data simulation, PEST software v.0.96 (NIEHS, 1996) was used.

In these experiments, we used SBP beads, and those for control were prepared with $CaCl_2$ (the equivalent to 0.20 mmol of the corresponding metal ion) instead

of copper acetate monohydrate in the hardening solution.

O_2 partial pressure measurement

In parallel with the ESR experiments, the measurements of O_2 partial pressure were made in triplicate with an O_2 sensor. For these experiments, ten SBP-beads were put into 9 mL of distilled water, and then 1 mL of 1.0 M H_2O_2 was added. The partial pressure of O_2 was measured before and after the addition of H_2O_2 with a NUMAK DO Analyzer, model JBP-607A, and a DO-957 Probe.

Methyl orange (MO) decolorization

The decolorization of the azo dye methyl orange (MO) by oxidation with H_2O_2 was studied with and without the presence of beads. In addition, the role of the entrapped enzyme SBP in the heterogeneous system was evaluated. For this purpose, the efficiency of beads with SBP was compared with the efficiency of beads without SBP.

In all cases, ten beads were used in combination with the selected volume of solution in order to measure the changes in absorbance at adequate time intervals. The experiments were performed in triplicate.

The study of MO decolorization efficiency followed two protocols:

- MO decolorization monitored after 8 h of reaction

In this case, an aliquot of 1.50 mL of 60 μM MO solution was put in contact with ten SBP-beads. Then, 50 mM H_2O_2 was added in aliquots of 100 μL with a frequency of one addition each 15 min, along 2.5 h to complete 1.0 mL (or 50 μmol of H_2O_2). The reaction took place under stirring, and, after 8 h, the beads were separated from the solution, washed with and kept in distilled water until next operative cycle. The resulting MO solution was analyzed by visible spectrophotometry. The H_2O_2 was added in this sequential way to prevent bubble formation inside the beads, which could eventually damage the assembly. A control was made with MO and H_2O_2 in the absence of the beads.

- MO decolorization kinetics

In this study, 2.00 mL of a solution containing 60 μM MO and 50 mM H_2O_2 were mixed with ten SBP beads. Aliquots of 200 μL were collected every 2 h, and were diluted with 500 μL of distilled water for immediate visible spectrophotometric analysis. A control was made with MO and H_2O_2 in the absence of beads. Another control was made using beads without the SBP enzyme inside.

Bacterial inhibition assay

The bacteria selected for this test was *Escherichia coli.* First, a bacterial suspension set in 10^5 CFU mL^{-1} was used to prepare the agar. Each type of bead was placed on an LB agar plate gel containing the bacteria, and the plate with all the beads was incubated at 37°C for 24 h. Then, the diameter of the bacterial inhibition zone was measured with a ruler in each case.

Results and discussion

Synthesis and characterization of EGDE-IM-MAA oligomers

This initial step in the synthesis of EGDE-IM-MAA oligomers started with the reaction of EGDE and IM for 24 h at 60° C to form the EGDE-IM adduct hydrogel (Lombardo Lupano et al. 2016), by opening of the epoxy groups present in the EGDE molecules due to the nucleophilic character of the nitrogen in the IM molecule. The adduct presented N_1-monosubstituted (IM) and N_1-N_3-disubstituted (IM^+) IM units which were, respectively, generated with a transient or permanent positive charge during the process. The N_1-monosubstituted IM units can be protonated with acidic solutions giving rise to IM protonated species (IMH^+), which are pH-sensitive (Scheme 1).

After the addition of the MAA monomer, the faster reaction was the formation of a ionic pair between MAA and monosubstituted IM (acid–base reaction in the EGDE-IM adduct hydrogel), and the slower reactions were the opening of the remaining epoxy groups to form esters of MAA, in parallel with the esterification of the hydroxyl groups in the EGDE-IM adduct by the carboxylic acid of MAA.

These oligomers were characterized by FT-IR and Raman spectroscopy (Fig. 1; Figs. S.1–S.3 in the Supporting Information). The FT-IR spectrum of the

Scheme 1 Chemical structure of sodium alginate, PEI.HCl and EGDE-IM-MAA oligomers

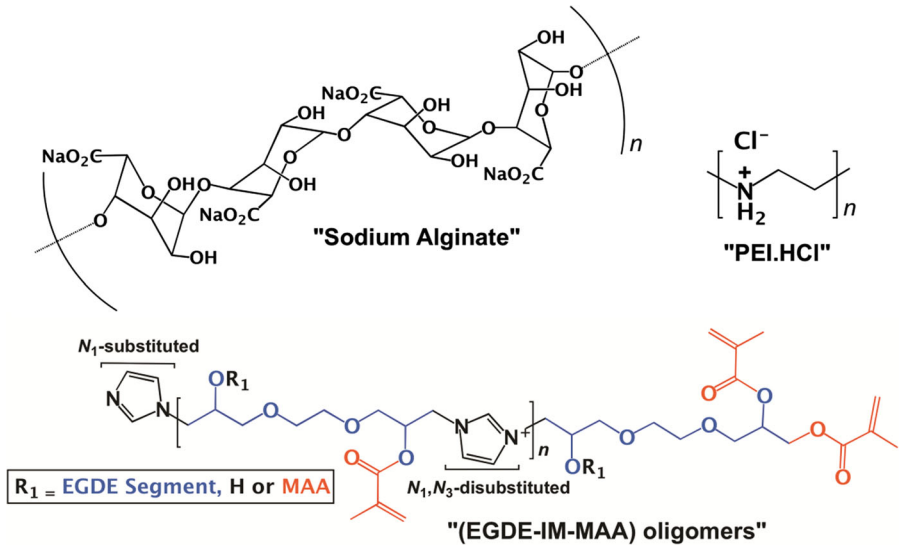

Fig. 1 FT-IR (*upper*) and Raman (*lower*) spectra of EGDE-IM-MAA oligomers

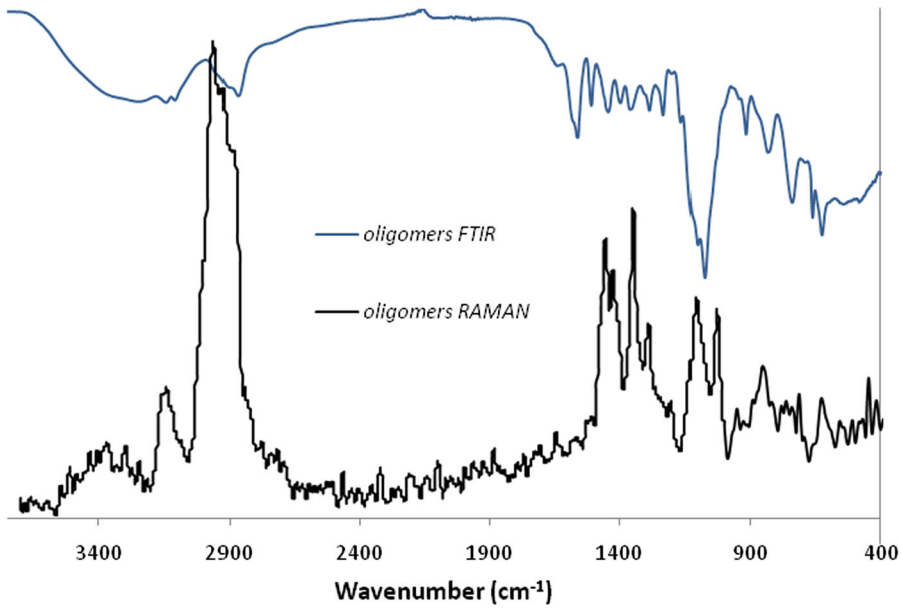

oligomers showed the typical vibrational bands at 663 and 835 (C=C and C=N), 1080 and 1106 (C–O–C), 1565 (C=C), 1510 (C=N), 1445 (aliphatic hydrocarbons and IM), 1360 and 1287 (δC–H), and 1234 cm^{-1} (C=N and δC–H), 3114 (N–H and sp^2 C–H), and 2873 cm^{-1} (sp^3 C–H) and 3250 cm^{-1} (O–H stretch) (Le et al. 2016). The absence of the oxirane band at 1253 cm^{-1}, and of the weak bands at 703, and 980 cm^{-1}, were indicative of epoxy ring opening from EGDE molecules by IM. The MAA mixed with EGDE-IM adduct was ionized by the formation of the ionic pair MA^- (EGDE-IMH^+), the reason why the C=O symmetric stretching band around 1690 cm^{-1} was absent.

The Raman spectrum of the oligomers presented bands broader than the signals from the corresponding monomers. Some signals in the product were associated with the structure of the corresponding EGDE, IM and MAA monomers (Figs. S.1–S.3 in the Supporting information). Other signals were exclusive of the oligomers, such as the band at 1030 cm^{-1}. Some of them seemed to be shifted as a consequence of the

chemical reaction (epoxy ring opening, *N*-substitution, and MAA esterification). In the same way, bands from the monomers were missing in the product. The strong band at 800 cm^{-1} in MAA was shifted to 856 cm^{-1} in the salt. The bands from MAA at 1640 and 1658 cm^{-1} corresponding to ν C=C were absent in the oligomer Raman spectrum, which could indicate that the amount of MAA residues bound to the oligomers was relatively low.

Concerning the presence of IM residues in the oligomers, the bands at 1090 and 1454 cm^{-1} could be assigned to aromatic rings, particularly aromatic azo. The last band, found in the oligomers and in the IM spectra, was also assigned to δCH_2 bound to *N* in disubstituted IM (IM^+) from ionic liquids (Moumene et al. 2015). In addition, the new band at 1030 cm^{-1} could be assigned to the $C(^+)H$ 0.p. bend from IM^+ (Markham et al. 1993). The strong Raman band at 1257 cm^{-1} in the EGDE spectrum corresponding to the oxirane ring vibration was absent in the spectrum of the product, as expected.

When the Raman spectrum of the oligomers was compared with the FT-IR spectrum, some signals of moderate to low intensity in the FT-IR were the strongest in the Raman (Fig. 1). The FT-IR peak at 1253 cm^{-1} corresponding to oxirane from EGDE, and a counterpart of the Raman peak at 1257 cm^{-1}, was absent in the product.

Cytotoxicity assays for EGDE-IM-MAA oligomers

The safety of these oligomers was tested following standard procedures with mammalian cells, and the results showed that the exposure of Vero cells to 10 mg L^{-1} oligomer solution did not lead to any significant decrease in cell viability when compared to their corresponding controls. In contrast, 20 mg L^{-1} and 40 mg L^{-1} of this compound produced a significant cell viability loss (> 70%).

According to these results, a set of 80 beads assembled with 60 mg of oligomers would be toxic for mammalian cells if these molecules were released in 1 L of solution. However a set of 10 beads hypothetically disrupted in 1 L of solution would release 7.5 mg of oligomers, and be innocuous.

Bead assembly

The adequate combination of sodium alginate, Ca(II), EGDE-IM-MAA oligomers, PEI.HCl and Cu(II) gave place to the alginate beads observed in Fig. 2, with particular properties.

One of the advantages of using oligomers is the fluidity imparted to the highly concentrated sodium alginate solution to be dispensed from a syringe. In this way, large amounts of the anionic polymer could be used to enhance the resistance to convection of the gel beads. When each drop of the viscous alginate solution fell into the less viscous PEI.HCl solution, a primary membrane was formed as a result of different possible physical and chemical processes: electrostatic attraction between $–COO^-$ residues from the drop, $–NH_3^+$/$–NRH_2^+$ from PEI.HCl, and H^+ exchange which induced the aggregation of the oligomer molecules. This primary membrane prevented the spherical drop from deforming and kept the alginate inside the bead. An ion exchange took place across this membrane between Na^+ from alginate and H^+ from the external solution. At the time that PEI.HCl diffused into the bead, the core underwent gradual gelation which was evidenced by an increase in the opacity. The intensity of this visual change

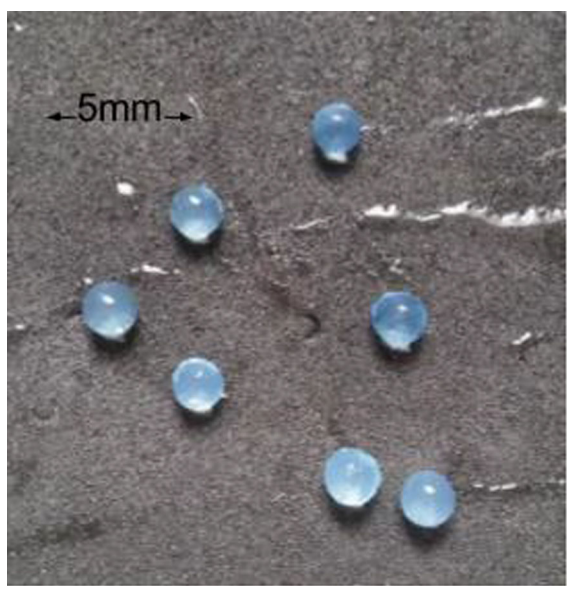

Fig. 2 Reinforced gel beads obtained from sodium alginate, EGDE-IM-MAA oligomers, $CaCl_2$, 22-kDa linear polyethylenimine hydrochloride (PEI.HCl) and copper acetate monohydrate

depended on the initial concentration of the oligomers in the internal solution.

In order to optimize the structural stability of the beads, different amounts of oligomers and PEI.HCl were tested, as shown in Table 1. The optimal amount of oligomer solution to fluidize the internal solution with alginate was at least 30 mg (100 μL from a 300-mg mL^{-1} solution). The PEI membrane was necessary to entrap the alginate and to provide structural stability to the beads, but the oligomer molecules bearing a positive electric charge were acting as a shield, weakening the interaction between $PEIH^{+}$ and alginate. This problem was overcome by increasing the amount of PEI.HCl in the external solution.

The preformed beads were stabilized by resting in Ca^{2+} solution for 1 h, after which they were transferred to the Cu(II)-hardening solution containing high amounts of Cu(II). The presence of inorganic anions at this point significantly affected the supra-structure assembly, the reason why the counterions acetate, tartrate or citrate were used instead of chloride or sulfate. Once the Cu(II) had penetrated the membrane and interacted with the macromolecules by coordination or electrostatic attraction, a shell was formed which provided high structural stability to the beads. The dimensions of the O30P20 beads were: diameter: 3.0 ± 0.4 mm; wet weight: 17 ± 1 mg; dry weight: 0.50 ± 0.03 mg; solid matter content: 8%; *n*: 10.

Beads characterization by Raman and FT-IR spectroscopies

The beads with Cu(II) could not be analyzed by Raman because the radiation induced the degradation of the material, so alternative beads were prepared with Ca(II) and Zn(II) instead of Cu(II). Those obtained with Ca(II) presented a spectrum similar to the spectrum of sodium alginate (Figs. S.4, S.5 in the Supporting Information), except for the absence of the band at 955 cm^{-1} from C–O–H deformation and C–C–H deformation, possibly indicating some changes in chain mobility of the polymer in the bead. A sharp peak at 1009 cm^{-1} was related to Ca(II).

On the other hand, the beads containing Zn(II) exhibited spectral bands from the alginate at 818, 833, 951 and 1095 cm^{-1}. In addition, the expected band from alginate C–H deformation at 1307 cm^{-1} was significantly weaker in the beads. The band at 1297 cm^{-1} was from PEI skeletal ν C–C, but those at 1146 and 1042 cm^{-1} from the same vibrations were missing (Fig. 3; Fig. S.6. in the Supporting Information).

The other bands from the beads were due to the oligomers, occurring at 1448, 1418, 1348, 1286, 1095, 1030, 951, 833, 713 and 444 cm^{-1}, but the band at 850 cm^{-1} was absent. Finally, the beads exhibited two new bands that did not come from the constitutive molecules: one at 1531 cm^{-1} that could be from ν C = C (perhaps enhanced by the presence of Zn(II)), and the other at 1237 cm^{-1} that could be from ν C–C chain vibration. In this way, the presence of alginate, oligomers and PEI in the beads was demonstrated by Raman spectroscopy, together with possible changes in chain mobility due to the assembly.

Concerning the FT-IR of the beads and their control structures without oligomers, most of the bands were from the alginate (Fig. S.7 in the Supporting Information). The band at 1083 cm^{-1} in the beads was stronger due to the contribution of the oligomers (C–

Table 1 Structural stability of each type of bead (OXPY) as a function of the amounts of oligomers and PEI.HCl, used in the internal and external assembly solutions, respectively

PEI.HCl	Oligomer			
	60 mg	30 mg	15 mg	0 mg
10 mg	O60P10: alginate leak and drop deformation	O30P10: good	O15P10: low alginate solution fluidity	O0P10: low alginate solution fluidity
20 mg	O60P20: good	O30P20: good	O15P20: good	O0P20: low alginate solution fluidity
30 mg	O60P30: good	O30P30: good	O15P30: good	O0P30: low alginate solution fluidity

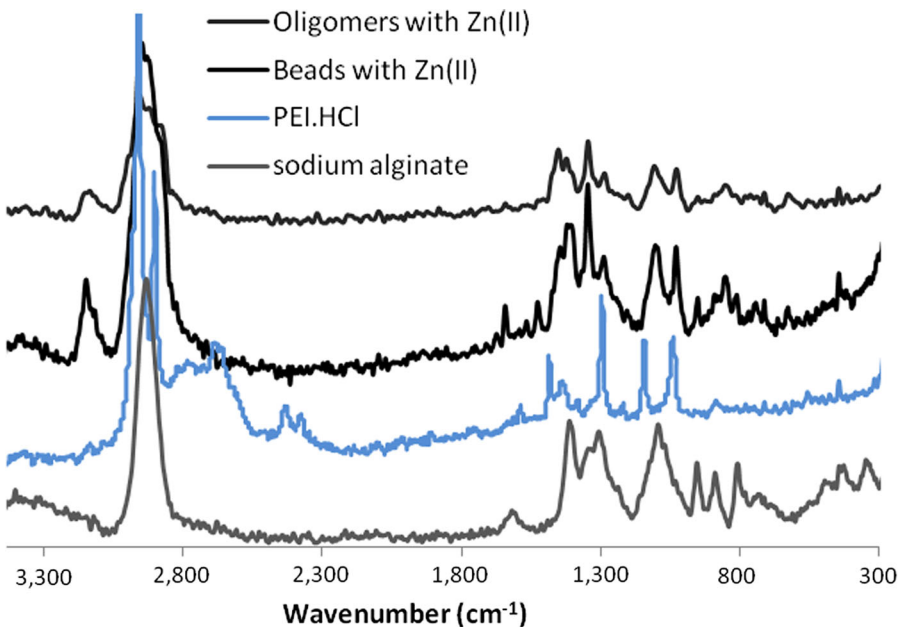

Fig. 3 Raman spectra of EGDE-IM-MAA oligomers interacting with Zn(II) (*upper*), beads stabilized and hardened with Zn(II) instead of Cu(II), PEI.HCl, and sodium alginate (*lower*)

O–C) and PEI (C–N). In addition, the band between 2960 and 2850 cm^{-1} (C–H stretch) was less resolved when the oligomers were included in the structure.

SEM images of the beads and elemental analysis by EDAX

As can be seen in Fig. 4 and Fig. S.8.A in the Supporting Information, the structural image of the beads showed that the combinations of reagents shown in Table 1 gave place to an internal core surrounded by an external shell, which often became detached from

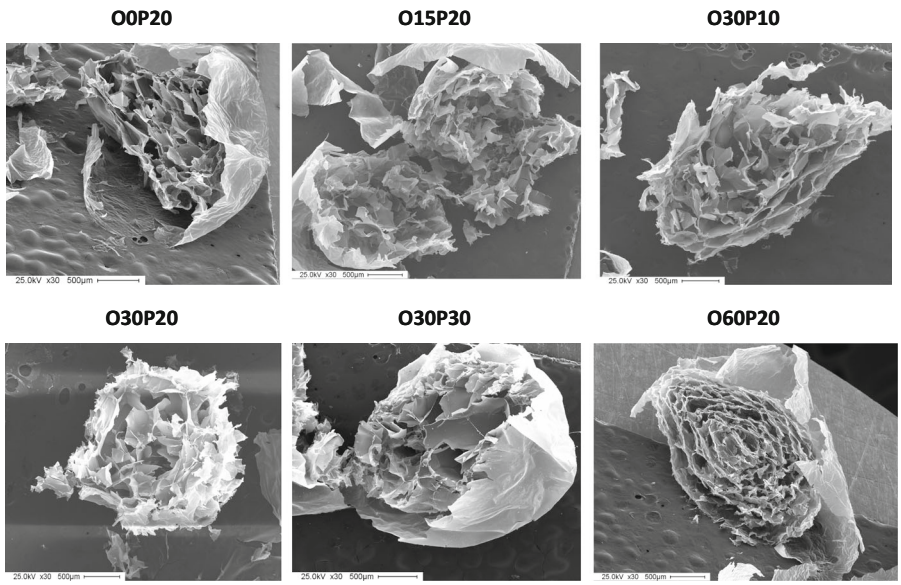

Fig. 4 SEM images of the lyophilized OXPY beads

the core by lyophilization. The core had a particular sponge-like tridimensional structure under that condition, with a porous network formed by the interaction between alginate, cations and oligomers. The addition of oligomers and/or PEI.HCl in different proportions did not alter the overall structure of the material when the oligomers were present in 30 mg (O30) or lower amounts in the internal solution. Instead, with 60 mg of oligomers (O60), a more organized assembly of the core was achieved. In this last case, the core structure seemed to be ordered in successive layers or hollow spheres (a cabbage-like structure), one inside the other, probably kept attached by molecular bridges. Thus, it can be said that the structure of the beads was mostly given by the alginate, which only altered its random conformation by interaction with an excess of oligomers. This could lead us to think that the interactions between the metal ions and the oligomers in excess brought a higher order of alginate chains.

Taking into account the mapping made by EDAX (Fig. S.8.B in the Supporting Information), it could be inferred that the distribution of the elements was homogeneous throughout the volume of most types of beads. To quantify this observation, calcium and copper, the elements which took part in the hardening process, were taken as a reference in the elemental zonal analysis of the beads showing nearly equal amounts in the center and the outermost areas. This fact could imply that ions may diffuse freely through the bead pores, providing a homogeneous hardening.

Nevertheless, the elemental analysis by EDAX (Table S.1 in the Supporting Information) was more sensitive with regard to ion distribution. A peculiar behavior was observed for the internal section of the O30P20 and O0P20 beads, which significantly differed from the others in their atom %, being particularly rich in copper and calcium. That amount of PEI.HCl in the outer layer would have determined a better interaction of alginate with inorganic ions in the core.

On the other hand, the proportion of copper and calcium was clearly higher in the external shell of the beads O30P30 and O60P20 than in the other samples. In the cases under study, the samples with higher amounts of PEI.HCl, in combination with certain amounts of oligomers, would determine higher proportions of copper and calcium in different strata of the beads.

In traditional Ca(II)-alginate gel beads, the non-uniform distribution of polymers is strongly dependent on alginate concentration, molecular size and the concentration of Ca(II) in the outer solution. Inhomogeneity is found when the diffusion of free alginate molecules in the gel phase is not restricted, and/or when the Ca(II) concentration is low (Skjåk-Bræk et al. 1989; Mikkelsen and Elgsaeter 1995). In our reinforced beads, the Ca(II) gradient was not evident from the EDAX results. Instead, the cation density was higher in the core or in the surface under certain PEI/oligomer combinations. According to these results, the differences in reagent diffusivity between standard and reinforced beads seem to be related to the assembly strategies; in the last case, Ca(II) and Cu(II) interacted with the polymers in the preformed beads, while in the traditional case, Ca(II) is the gelling cation producing a concentration gradient from the surface to the bead core.

Structural stability tests and texturometric assays

In the last stage of hardening, a shell was formed as a result of the interactions of Cu(II) with the macromolecules, providing high structural stability and stress resistance to the beads. Different tests were performed to verify these properties. The physical integrity towards convection was analyzed by keeping the beads in distilled water under stirring at maximal speed for 72 h, and none of the ten O30P20 samples was broken under this treatment. The replacement of water by a 3.5% NaCl solution under stirring did not produce any effects on their integrity. The beads also resisted the free fall from 1.5 m of height.

Then, the different types of beads were sonicated to test the structural stability of each assembly towards vibration. The results shown in Fig. 5 clearly indicate that the most friable were those beads with the lowest oligomer content, and the most resistant to vibration were those with the highest amount of oligomer. After 90 min of sonication, the amount of intact O60P20 beads was significantly higher than the amount of intact O15P20 beads ($p < 0.05$). After 120 min of sonication, the amount of intact O60P20 beads was significantly higher than the amount of intact O30PY beads ($p < 0.05$). In this way, the overall results proved that the beads rich in oligomers were particularly resistant to convection, vibration and free fall.

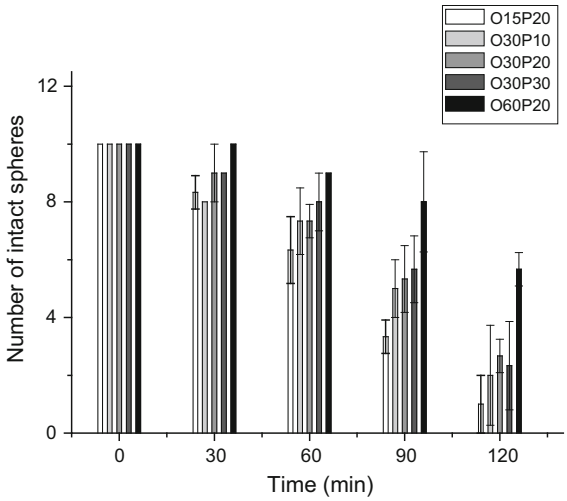

Fig. 5 Number of intact OXPY beads as a function of time of sonication

The mechanical properties of the structurally stable beads were studied. The texturometric parameter hardness is related to the resistance of the gel bead to compression, and the parameter cohesiveness is related to the difficulty in breaking down the internal structure of the bead (Dini et al. 2014).

Table S.1 in the Supporting Information exhibits the estimated parameters for each type of bead. Concerning cohesiveness, there was no significant difference between the mean values of the tested groups ($p > 0.01$), indicating that this type of test was not sensitive enough to demonstrate the effect of the oligomers on the internal structure stability. On the other hand, the homogeneous degree of cohesiveness could be associated with the alginate and its degree of hydration. Alginate was the main component of the matrix but it could also be added in high proportions to the internal solution due to the positive effect of the oligomers on fluidity.

The tested bead matrixes showed no significant differences in hardness ($p > 0.01$), except for O30P30 ($p < 0.01$) with a mean value almost 50% higher. These results demonstrate the relevance of the amount of PEI in the shell on bead firmness.

The intermolecular reticulation between PEI, alginate and oligomers created a surrounding shell and a stable core matrix with high resistance to vibration and compression. PEI also imparted higher cation uptake capacity to the beads and this property was closely related to the higher hardness value. In fact, in the external shell of the bead O30P30, the proportion of copper and calcium was clearly higher than in the other samples.

Free radicals detection by ESR, and O_2 detection

The SBP enzyme was immobilized in the reinforced beads to be used as a catalytic oxidative system in the presence of H_2O_2 on dye decolorization. The Cu(II) entrapped in the matrix was expected to activate H_2O_2 with the release of O_2 and free radicals, which would contribute to the oxidative process catalyzed by SBP (Lázaro Martínez et al. 2008). In fact, the SBP beads/H_2O_2 heterogeneous system produced free radicals which diffused into the solution and were detected by ESR spin-trapping experiments with a DMPO spin-trap. The simulated spectrum of Fig. 6 fitted well with the experimental spectrum, and was the sum of two different radical adducts: DMPO/OH and DMPO/C from a hydroxyl radical ($OH^{\cdot}$) and from a carbon-centered free radical, respectively. These species were assigned on the basis of the hyperfine coupling constants obtained from simulation (Guo et al. 2003), and are listed in Table S.2 in the Supporting Information.

A series of control experiments were performed to determine the source of these free radicals. Some beads were assembled using only Ca(II) instead of Cu(II), and no free radicals were detected with DMPO as spin-trap, after H_2O_2 addition. Also, neither the

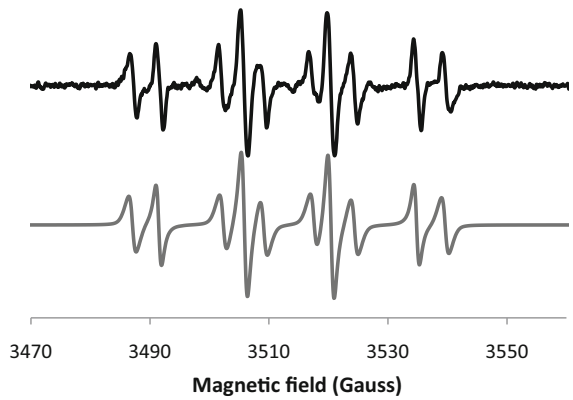

Fig. 6 ESR spectrum (*upper*) and simulated spectrum (*lower*) on H_2O_2 activation by the O60P20 SBP-beads, after 10 min of reaction. Spin-trap: DMPO. Correlation coefficient on simulation (R): 0.952

oligomers in the beads nor SBP participated in the release of free radicals.

A PEI.HCl solution in contact with H_2O_2 produced $OH^{\cdot}$, which was also detected when the heterogeneous Cu(II)-PEI/H_2O_2 system was tested. The peroxide itself in the presence of DMPO also evidenced some release of free radicals (Fig. S.9 in the Supporting Information).

These results indicated that the H_2O_2 was mostly activated by the Cu(II) sites in the beads. Even if the PEI molecules dissolved in acidic medium favored the release of $OH^{\cdot}$ from H_2O_2, the polymer itself provided few catalytic sites for H_2O_2 activation in the beads because a fraction of the basic functional groups were forming complexes with Cu(II). Thus, the catalytic sites in the beads for H_2O_2 activation are expected to be Cu(II)-alginate, Cu(II)-PEI and/or Cu(II)-oligomers.

The abundant carbon-centered free radicals might have originated from the reaction of $OH^{\cdot}$ with alginate molecules in the core of the beads. The possible reaction of H_2O_2 activation catalyzed by non-soluble Cu(II)-complexes, has been studied and presented in previous reports (Lázaro-Martínez et al. 2016):

$$3H_2O_2 \rightleftarrows O_2 + 2OH^{\cdot} + 2H_2O$$

In order to detect the production of O_2, the partial pressure was measured in the SBP-beads/H_2O_2 heterogeneous system before and after the addition of H_2O_2. The release of gas upon H_2O_2 addition was instantaneous, and the concentration after 30 min of reaction registered an increase of 60% (Fig. S.10 in the Supporting Information). When H_2O_2 was added to the system containing SBP beads without Cu(II), the O_2 partial pressure did not increase, confirming that the release of O_2 was related to the presence of Cu(II) in the beads. However, the structural stability of the beads was strongly affected by O_2 release after H_2O_2 addition. When the spheres were put in solutions with H_2O_2 concentrations higher than 0.1 M, the structures experienced breaking off due to bubble productions at Cu(II) sites.

Methyl orange (MO) decolorization

The identification of reactive oxygen species on H_2O_2 activation by the beads was indicative of their applicability as a catalyst on degradative processes. In order to examine this potential, the SBP beads were tested in the decolorization of MO, an azo dye whose degradation products are well known and described in the literature (Chen et al. 2001; Baiocchi et al. 2002).

The enzyme SBP was specially encapsulated in the beads for this application, with the aim of enhancing the oxidative efficiency of the heterogeneous system. This biomolecule, extracted from the seed-coat (a by-product from food industry), catalyzes the oxidation of organic substrates by H_2O_2, and is very stable and abundant in nature. From the different strategies assayed, two protocols were proved adequate for MO oxidation.

In the first attempt, the dye oxidation with H_2O_2 was carried out in both heterogeneous (in the presence of the O30P20 SBP beads) and homogeneous (in the absence) systems, and the results were analyzed after 8 h of reaction. The final MO concentration was 22.9 μM in the heterogeneous system, but was 35.7 μM in the homogeneous systems free of catalyst serving as control. The Cu(II) was expected to activate the release of free radicals, and SBP entrapped in the beads was expected to catalyze the oxidation of MO, enhancing the efficiency of the decolorization process. ESR complementary studies had already demonstrated that SBP did not release any free radicals, as expected (data not shown).

These beads were recovered to evaluate the stability of the catalyst on recycling. After a second operative cycle on a fresh MO solution, the dye final concentration was 25.7 μM, and after a third operative cycle it was 28.7 μM. The relative values of this experiment indicated that the decolorization was 36% after the first operative cycle, when 50 μmol of H_2O_2 were added in steps to 0.09 μmol of MO for 2.5 h. The subsequent operative cycles were less efficient at 28 and 20%, indicating that some catalytic sites had been inactivated or even lost on re-use (Fig. S.11 in the Supporting Information).

In the second approach, a kinetic study was performed using higher H_2O_2 concentration. In order to examine the enhanced oxidation by the catalysts in the beads, the MO concentration in the heterogeneous system was normalized by the MO concentration in the homogeneous system free of catalyst. Table 2 shows the $[MO]_{reaction}/[MO]_{control}$ ratio as a function of time for different heterogeneous systems (the control was performed in a homogeneous system free of any catalyst). It was evident that all the assemblies were clearly more efficient than the control without

Table 2 MO concentration normalized by control ($[MO]_{reaction}/[MO]_{control}$), as a function of reaction time in the heterogeneous system containing H_2O_2 and OXPY SBP beads

Time	$[MO]_{reaction}/[MO]_{control}$[a]						
(h)	O0P20	O15P20	O30P10	O30P20	O30P30	O60P20	Control
0	1.21	1.18	1.16	1.16	1.36	1.23	1.00
2	0.96	0.77	0.83	0.76	0.58	0.82	1.00
4	0.84	0.73	0.87	0.86	0.84	0.45	1.00
6	0.50	0.33	0.30	0.35	0.37	0.20	1.00
8	0.44	0.20	0.23	0.21	0.24	0.09	1.00

The control was made with the homogeneous system (MO and H_2O_2)

[a]The RSD of MO concentrations was lower than 10% in all cases

catalysts on MO decolorization. The O60P20 SBP beads (with the highest amount of oligomers) presented the highest activity on MO oxidation by H_2O_2, because the dye concentration normalized by control gradually decreased as a function of time, removing 91% (compared with the control) after 8 h of treatment. In addition, the slowest heterogeneous system was O0P20, where the oligomers were absent. In this way, the relevance of these synthetic EGDE-IM-MAA oligomers on the catalytic process of dye removal was clearly demonstrated.

In parallel, a batch of beads was prepared without SBP (Table S.3 in the Supporting Information). In the absence of the enzyme, the MO normalized concentrations differed from the MO in the homogeneous system free of any catalyst, but the efficiency of decolorization was significantly lower. In this way, the activity of SBP in the heterogeneous system on MO removal was evidenced: the dye would be co-substrate of this peroxidase, and was oxidized by H_2O_2. These results would indicate that the synthetic EGDE-IM-MAA oligomers acted as SBP stabilizers on the catalytic process of dye removal (Torres et al. 2017). The actions of the free radicals produced in the presence of Cu(II) were evident, but their contribution on decolorization was less significant.

Bacterial inhibition assay

The cation release activity was also studied with Cu(II)-hardened beads by antimicrobial activity assay. Figure S.12 in the Supporting Information shows that the bacteria was allowed to grow in the agar medium for 24 h in the presence of beads of different composition. The inhibition zone around each bead indicated the antimicrobial activity of the material under test. The results in Table S.4 in the Supporting Information demonstrated that the presence of Cu(II) was responsible for wide rings of no bacterial growth. Instead, the bead in the center made without Cu(II) in the hardening step showed no change at all in the surrounding bacterial concentration.

The inhibition effect could be attributed to Cu(II) leakage and/or antimicrobial free radicals release from Cu(II) sites in the beads. Complexed Cu(II) can activate dissolved O_2 for the production of oxidizing free radicals, as was demonstrated in a previous work (Lázaro-Martínez et al. 2016). These reactive species could diffuse in the agar and prevent bacterial growth. On the other hand, Cu(II) itself released from the beads and diffusing in agar can act as an antimicrobial agent. Microbeads of copper–alginate hydrogels induced immediate bactericidal effects against *Escherichia coli* and *Staphylococcus aureus* (Malagurski et al. 2016). The bead made without Cu(II) did not inhibit bacterial growth, indicating that the amount of oligomers released from the bead was innocuous, consistent with the results of cytotoxicity assays.

Conclusions

The adequate combination of sodium alginate, EGDE-IM-MAA oligomers, PEI.HCl, Ca(II) and Cu(II) produced structurally stable beads towards convection, vibration and free fall. The ionotropic gelation of the reactants followed by metal ion hardening, induced intermolecular reticulation originating a stable matrix with high resistance to stirring and sonication. Moreover, the coordination properties of the oligomers

allowed the spheres to retain their structure in Ca(II)-free media without the need of covalent cross-linking.

EDAX results indicated that the distribution of Ca(II) and Cu(II) was homogeneous in the overall structure. The amount of PEI.HCl in combination with certain proportions of oligomers determined higher amounts of cations in different bead strata, and this combination of higher PEI and cations was directly associated with higher bead hardness.

The PEI molecules formed a shell which completely surrounded each bead. The synthetic oligomers had multiple roles in the assemblies, being particularly important for the increase of fluidity of alginate solutions which favored the use of higher amounts of this polysaccharide. SEM images demonstrated that the amount of oligomers determined the orientation of alginate chains in the core of the beads. This reticulated structure associated with the presence of oligomers would impart an increased structural stability to the beads.

The synergistic combination of the immobilized enzyme SBP and complexed Cu(II) in the beads was effective on dye removal by oxidation with H_2O_2 from aqueous solution. The amount of oligomers entrapped in the beads played a crucial role in the efficiency of the treatment in those assemblies containing the peroxidase. These synthetic molecules bearing IM units acted in stabilizing the enzyme, perhaps protecting the molecules from harsh conditions and certainly retaining the protein in the matrix. H_2O_2 was activated by Cu(II)-complexes, releasing free radicals and O_2, but the sole action of the catalytic Cu(II)-sites did not explain the huge removal of the dye by SBP beads/H_2O_2 heterogeneous system.

The bacterial growth inhibition was directly related to the presence of Cu(II) complexes. This cation can activate dissolved O_2 for the production of oxidizing free radicals, as was demonstrated in a previous work. The oligomer cytotoxicity on cell culture was dependent on their concentration, but the beads containing oligomers did not show harmful effects on bacterial cells.

In this simple way, we obtained gel beads with outstanding resistance to different treatments: stirring, vibration and fall. The chemical resistance was also demonstrated on H_2O_2 addition at concentration levels below 0.1 M, but, at higher amounts, the O_2 bubbles produced disruption of the structure. The beads containing peroxidase and Cu(II) sites proved to be adequate catalysts for oxidation processes in environmental matters.

Acknowledgments The authors gratefully acknowledge the financial support from Universidad de Buenos Aires (UBACyT 11-14/915, 13-16/780 and 13-16/021), CONICET (10-12/PIP 076, 12-14/PIP 657 and 14-16/PIP 130), and ANPCyT (BID PICT 2012-0716). D.I.T. thanks the CONICET for his doctoral fellowship. Dr. M. E. V. thanks the CONICET for her post-doctoral fellowship. The authors thank Dr. M. L. Cuestas for the cytotoxicity assays, Prof. M. V. Miranda for the SBP extracts, and Prof. L.L. Piehl for her contribution in ESR experiments.

References

Anu PR, Bijoy Nandan S, Jayachandran PR, Don Xavier ND (2016) Toxicity effects of copper on the marine diatom, Chaetoceros calcitrans. Reg Stud Mar Sci 8(3):498–504. https://doi.org/10.1016/j.rsma.2016.07.001

Ates S, Cortenlioglu E, Bayraktar E, Mehmetoglu U (2007) Production of L-DOPA using Cu-alginate gel immobilized tyrosinase in a batch and packed bed reactor. Enzyme Microb Technol 40(4):683–687. https://doi.org/10.1016/j.enzmictec.2006.05.031

Baiocchi C, Brussino MC, Pramauro E, Bianco Prevot A, Palmisano L, Marcí G (2002) Characterization of methyl orange and its photocatalytic degradation products by HPLC/UV–VIS diode array and atmospheric pressure ionization quadrupole ion trap mass spectrometry. Int J Mass Spectrom 214:247–256

Bourne MC, Comstock SH (1981) Effect of degree of compression on texture profile analysis. J Texture Stud 12:201–216. https://doi.org/10.1111/j.1745-4603.1981.tb01232.x

Chen F, Xie Y, He J, Zhao J (2001) Photo-Fenton degradation of dye in methanolic solution under both UV and visible irradiation. J Photochem Photobiol A 138:139–146

Cheng ZW, Chen JM, Chen DZ, Zhang LL (2011) Biodegradation of methyl tert-butyl ether in a bioreactor using immobilized *Methylibium petroleiphilum* PM1 cells. Water Air Soil Pollut 214:59–72. https://doi.org/10.1007/s11270-010-0403-3

Cui J, van Koeverden MP, Müllner M, Kempe K, Caruso F (2014) Emerging methods for the fabrication of polymer capsules. Adv Colloid Interface Sci 207:14–31. https://doi.org/10.1016/j.cis.2013.10.012

Dini C, Islan GA, Castro GR (2014) Characterization and stability analysis of biopolymeric matrices designed for phage-controlled release. Appl Biochem Biotechnol 174:2031–2047. https://doi.org/10.1007/s12010-014-1152-3

Guo Q, Qian SY, Mason RP (2003) Separation and identification of DMPO adducts of oxygen-centered radicals formed from organic hydroperoxides by HPLC-ESR, ESI-MS and MS/MS. J Am Soc Mass Spectrom 14(8):862–871. https://doi.org/10.1016/S1044-0305(03)00336-2

Homaei AA, Sariri R, Vianello F, Stevanato R (2013) Enzyme immobilization: an update. J Chem Biol 6(4):185–205. https://doi.org/10.1007/s12154-013-0102-9

Kawaguti HY, Buzzato MF, Castilho Orsi D, Tiemi Suzuki G, Sato HH (2006) Effect of the additives polyethylenimine and glutaraldehyde on the immobilization of *Erwinia sp*. D12 cells in calcium alginate for isomaltulose production. Process Biochem 41:2035–2040. https://doi.org/10.1016/j.procbio.2006.05.003

Kocaturk S, Yagar H (2010) Optimization of polyphenol oxidase immobilization in copper alginate beads. Artif Cells Blood Substit Immobil Biotechnol 38(3):157–163. https://doi.org/10.3109/10731191003790406

Kurillova L, Gemeiner P, Vikartovska A, Mikova H, Rosenberg M, Ilavsky M (2000) Calcium pectate gel beads for cell entrapment. 6. Morphology of stabilized and hardened calcium pectate gel beads with cells for immobilized biotechnology. J Microencapsul 17(3):279–296. https://doi.org/10.1080/026520400288265

Lázaro Martínez JM, Leal Denis MF, Piehl LL, Rubín de Celis E, Buldain GY, Dall' Orto VC (2008) Studies on the activation of hydrogen peroxide for color removal in the presence of a new Cu(II)-polyampholyte heterogeneous catalyst. Appl Catal B 82:273–283. https://doi.org/10.1016/j.apcatb.2008.01.030

Lázaro-Martínez JM, Rodríguez-Castellón E, Vega D, Monti GA, Chattah AK (2015) Solid-state studies of the crystalline/amorphous character in linear poly(ethylenimine hydrochloride) (PEI·HCl) polymers and their copper complexes. Macromolecules 48(4):1115–1125. https://doi.org/10.1021/ma5023082

Lázaro-Martínez JM, Lombardo Lupano LV, Piehl LL, Rodríguez-Castellón E, Dall' Orto VC (2016) New insights about the selectivity in the activation of hydrogen peroxide by cobalt- or copper-hydrogel heterogeneous catalysts in the generation of reactive oxygen species. J Phys Chem C 120(51):29332–29347. https://doi.org/10.1021/acs.jpcc.6b10957

Le TT, Murugesan K, Lee CS, Vu CH, Chang TS, Jeon JR (2016) Degradation of synthetic pollutants in real wastewater using laccase encapsulated in core–shell magnetic copper alginate beads. Bioresour Technol 216:203–210. https://doi.org/10.1016/j.biortech.2016.05.077

Lee PM, Lee KH, Siaw YS (1993) Immobilization of aminoacylase in polyethylenimine stabilized calcium alginate beads for L-phenylalanine production. Biomater Artif Cells Immobil Biotechnol 21(4):563–570. https://doi.org/10.3109/10731199309117658

Lombardo Lupano LV, Lázaro-Martínez JM, Vizioli NM, Torres DI, Dall' Orto VC (2016) Synthgation behavior and formation of hollow spheres. Macromol Mater Eng 301(2):167–181. https://doi.org/10.1002/mame.201500276

Malagurski M, Vukasinovic-Sekulic M, Kostic D, Levic S (2016) Towards antimicrobial yet bioactive Cu-alginate hydrogels. Biomed Mater 11:035015. https://doi.org/10.1088/1748-6041/11/3/035015

Markham LM, Mayne LC, Hudson BS, Zgierski MZ (1993) Resonance Raman studies of imidazole, imidazolium, and their derivatives: the effect of deuterium substitution. J Phys Chem 40:10319–10325. https://doi.org/10.1021/j100142a010

Mikkelsen A, Elgsaeter A (1995) Density distribution of calcium-induced alginate gels: a numerical study. Biopolymers 36(1):17–41. https://doi.org/10.1002/bip.360360104

Mogharabi M, Nassiri-Koopaei N, Bozorgi-Koushalshahi M, Nafissi-Varcheh N, Bagherzadeh G, Faramarzi MA (2012) Immobilization of laccase in alginate-gelatin mixed gel and decolorization of synthetic dyes. Bioinorg Chem Appl. https://doi.org/10.1155/2012/823830

Moumene T, Belarbi EH, Haddad B, Villemin D, Abbas O, Khelifa B, Bresson S (2015) Study of imidazolium dicationic ionic liquids by Raman and FTIR spectroscopies: the effect of the nature of the anion. J Mol Struct 1083:179–186. https://doi.org/10.1016/j.molstruc.2014.11.061

Nisha S, Karthick A, Gobi N (2012) A review on methods, application and properties of immobilized enzyme. Chem Sci Rev Lett 1(3):148–155 **(Article CS17204211)**

Nussinovitch A (2010) In: Polymer macro- and micro-gel beads: fundamentals and applications. Springer, New York. ISBN:978-1-4419-6618-6

Paul T, Jana A, Das A, Mandal A, Halder SK, Mohapatra PKD, Pati BR, Mondal KC (2014) Smart cleaning-in-place process through crude keratinase: an eco-friendly cleaning techniques towards dairy industries. J Clean Prod 76:140–153. https://doi.org/10.1016/j.jclepro.2014.04.028

Reddy N, Reddy R, Jiang Q (2015) Crosslinking biopolymers for biomedical applications. Trends Biotechnol 33(6):362–369. https://doi.org/10.1016/j.tibtech.2015.03.008

Santagapita PR, Mazzobre MF, Buera MP (2011) Formulation and drying of alginate beads for controlled release and stabilization of invertase. Biomacromol 12:3147–3155. https://doi.org/10.1021/bm2009075

Skjåk-Bræk G, Grasdalen H, Smidsrød O (1989) Inhomogeneous polysaccharide ionic gels. Carbohydr Polym 10(1):31–54. https://doi.org/10.1016/0144-8617(89)90030-1

Teerapatsakul C, Bucke C, Parra R, Keshavarz T, Chitradon L (2008) Dye decolorisation by laccase entrapped in copper alginate. World J Microbiol Biotechnol 24:1367–1374. https://doi.org/10.1007/s11274-007-9617-y

Torres DI, Miranda MV, Dall' Orto VC (2017) One-pot preparation of SBP-PANI-PAA-ethylene glycol diglycidyl ether sensor foe electrochemical detection of H_2O_2. Sens Actuat B 239:1016–1025. https://doi.org/10.1016/j.snb.2016.08.110

Traffano-Schiffo MV, Aguirre Calvo TR, Castro-Giraldez M, Fito PJ, Santagapita PR (2017) Alginate beads containing lactase: stability and microstructure. Biomacromolecules 18:1785–1792. https://doi.org/10.1021/acs.biomac.7b00202

Trivedi UJ, Bassi AS, Zhu J (2006) Investigation of phenol removal using sol–gel/alginate immobilized soybean seed hull peroxidase. Can J Chem Eng 84(2):239–247. https://doi.org/10.1002/cjce.5450840211

Xu DY, Yang Z (2013) Cross-linked tyrosinase aggregates for elimination of phenolic compounds from wastewater. Chemosphere 92(4):391–398. https://doi.org/10.1016/j.chemosphere.2012.12.076

Xue YP, Xu M, Chen HS, Liu ZQ, Wang YJ, Zheng YG (2013) A novel integrated bioprocess for efficient production of (R)(−)-mandelic acid with immobilized *Alcaligenes faecalis* ZJUTB10. Org Process Res Dev 17:213–220. https://doi.org/10.1021/op3001993